

# Inhibition of the Anatase–Rutile Phase Transformation with Addition of CeO<sub>2</sub> to CuO–TiO<sub>2</sub> System: Raman Spectroscopy, X-ray Diffraction, and Textural Studies

Maria Suzana P. Francisco\* and Valmor R. Mastelaro

Departamento de Física e Ciência dos Materiais, Instituto de Física de São Carlos, Universidade de São Paulo, P.O. Box 369, 13560-970, São Carlos SP, Brazil

Received October 29, 2001. Revised Manuscript Received March 5, 2002

The effect of the addition of CeO<sub>2</sub> on the structural and textural properties of TiO<sub>2</sub> and TiO<sub>2</sub>–CuO samples calcined at different temperatures was analyzed. The structural and textural transformation when the temperature of calcination was varied was followed by X-ray diffraction, Raman spectroscopy, and N<sub>2</sub> adsorption techniques. The addition of CeO<sub>2</sub> to the TiO<sub>2</sub> and TiO<sub>2</sub>–CuO samples decreases the anatase–rutile phase transformation when compared with the case of pure TiO<sub>2</sub>. This decrease observed for the phase transformation prevents the substantial surface loss and pore growth associated with this process.

## Introduction

Titania (TiO<sub>2</sub>) has been widely studied due its interesting properties such as high dielectric constant, humidity, and oxygen sensitivities and photoelectric and catalytic conversion properties.<sup>1,2</sup>

Copper supported on TiO<sub>2</sub> presents interesting properties in the field of heterogeneous catalysis and has been widely used in the industry for selective oxidation of *o*-xylene to phthalic anhydride,<sup>3,4</sup> steam reforming and methanol dehydrogenation,<sup>5,6</sup> CO oxidation,<sup>7,8</sup> NO<sub>x</sub> decomposition,<sup>7</sup> and complete mineralization of a variety of volatile organic compounds (VOCs).<sup>9</sup>

Titania crystallizes in three natural phases: brookite (orthorhombic), anatase (tetragonal), and rutile (tetragonal). The brookite and anatase crystalline phases, which are stable at low temperature, transform into rutile when the sample is calcined at higher temperatures.<sup>10</sup> However, brookite and anatase can be stabilized at high temperatures if dopants are present during synthesis, inhibiting their transformation into rutile.<sup>11–13</sup>

It has been demonstrated that some properties of TiO<sub>2</sub> are very sensitive to its structure. Since the anatase phase is chemically and optically active, it is suitable for catalysts and supports.<sup>14,15</sup> On the other hand, the

rutile phase has the highest refractive index and ultraviolet absorptivity among the titania phases; thus, it is employed in pigments, paints, ultraviolet absorbents.<sup>14</sup>

According to the temperature, the anatase–rutile transformation is related to some extent with the degree of packing of the particles, since the transformation begins with the nucleation of rutile on anatase and the rutile nuclei grow throughout the anatase particle until completion.<sup>14</sup> High surface area titania is commonly formed by the metastable anatase phase which, upon heating at temperatures above 800 K, transforms into the more stable rutile form with extensive surface area loss.<sup>14,15</sup> Since anatase is a metastable TiO<sub>2</sub> polymorph, it tends to transform into the rutile phase, decreasing the surface area, inducing a loss of catalytic activity.<sup>16</sup>

The anatase–rutile transformation was found to be a major cause of deactivation in vanadio–titania oxidation catalysts.<sup>17</sup> Anatase shows a better performance in photocatalysis than rutile.<sup>18</sup> It has been found that a 70/30 anatase/rutile mix makes the best photocatalyst for the oxidation of organics in wastewater. The anatase phase is found to have a better performance as a support of V<sub>2</sub>O<sub>5</sub>/TiO<sub>2</sub> for selective partial oxidation reactions, relative to the pure rutile phase.<sup>19</sup>

The stabilization of TiO<sub>2</sub> in the anatase phase can usually be achieved by changing its bulk or surface composition, and as mentioned before, it is usual to add other atoms to titania in order to improve TiO<sub>2</sub> properties such as structural stability. It has been reported that CeO<sub>2</sub> has the property of stabilizing the active phase in a fine dispersed state and improving the resistance to thermal loss of the supported catalyst surface area and the catalytic activity.<sup>21–23</sup>

- \* To whom correspondence should be addressed. E-mail: suzana@iqm.unicamp.br.
- (1) Bersani, D.; Lottici, P. P.; Ding, X. Z. *Appl. Phys. Lett.* **1998**, *72*, 73.
- (2) Wijnhoven, J. E. G. J.; Vos, W. L. *Science* **1998**, *281*, 802.
- (3) Busca, G.; Ramis, G.; Gallardo-Amores, J. M.; Escribano, V. S.; Piaggio, P. *J. Chem. Soc., Faraday Trans.* **1994**, *90*, 3181.
- (4) Wainwright, M. S.; Foster, N. R. *Catal. Ver.* **1979**, *19*, 211.
- (5) Breen, J. P.; Ross, J. R. H. *Catal. Today* **1999**, *51*, 521.
- (6) Takezawa, N.; Iwasa, N. *Catal. Today* **1997**, *36*, 45.
- (7) Larsson, P.-O.; Andersson, A. *Appl. Catal. B* **2000**, *24*, 175.
- (8) Dong, G.; Wang, J.; Gao, Y.; Chen, S. *Catal. Lett.* **1999**, *58*, 37.
- (9) Kumar, P. M.; Badrinarayanan, S.; Sastry, M. *Thin Solid Films* **2000**, *358*, 122.
- (10) Bokhimi, X.; Novaro, O.; Gonzalez, R. D.; López, T.; Chimal, O.; Asomoza, A.; Gómez, R. *J. Solid State Chem.* **1999**, *144*, 349.
- (11) Sánchez, E.; López, T.; Gómez, R.; Bokhimi, X.; Morales, A.; Novaro, O. *J. Solid State Chem.* **1996**, *122*, 309.
- (12) Zaspalis, V. T.; Van Praag, W.; Keizer, K.; Ross, J. R. H.; Burggraaf, A. J. *J. Mater. Sci.* **1995**, *27*, 1023.
- (13) Shannon, R. D.; Pask, J. A. *J. Am. Ceram. Soc.* **1965**, *48*, 391.

- (14) Xia, B.; Huang, H.; Xie, Y. *Mater. Sci. Eng. B* **1999**, *57*, 150.
- (15) Fogar, K.; Anderson, J. R. *Appl. Catal.* **1986**, *23*, 139.
- (16) Gallardo-Amores, J. M.; Escribano, V. S.; Busca, G.; Lorezelli, V. *J. Mater. Chem.* **1994**, *4*, 965.
- (17) Saleh, R. Y.; Wachs, I. E.; Chan, S. S.; Chersich *J. Catal.* **1986**, *98*, 102.
- (18) Augustynski, J. *Electrochim. Acta* **1993**, *38*, 43.
- (19) Deo, G.; Turek, A. M.; Wachs, I. E.; Machej, T.; Haber, J.; Das, N.; Eckert, H.; Hirt, A. M. *Appl. Catal. A* **1992**, *91*, 27.
- (20) Berry, R. J.; Mueller, M. R. *Microchem. J.* **1994**, *50*, 28.

In this work, our goal is to study the anatase–rutile phase transformation after the addition of  $\text{CeO}_2$  into  $\text{TiO}_2$  and into  $\text{CuO–TiO}_2$  matrices prepared by the sol–gel process. To accomplish that goal, we employed physical absorption, X-ray diffraction (XRD), and Raman spectroscopy techniques.

## Experimental Section

**Sample Preparation.** The sol–gel method was employed to prepare titania-based mixed oxides. Commercial  $(\text{NH}_4)_2\text{Ce}(\text{NO}_3)_6$  powder (Vetec) was dissolved in an aqueous nitric acid solution (1.5 mol/L).  $\text{Cu}(\text{NO}_3)_2 \cdot 3\text{H}_2\text{O}$  powder (Vetec) was then added, heated to 80 °C, and kept at this temperature for 30 min. The resulting solution was called A. Another solution, called B, was prepared with tetraisopropyl orthotitanate ( $\text{C}_{12}\text{H}_{28}\text{O}_4\text{TiO}$ , Merck), which was dissolved in isopropyl alcohol (mole ratio = 1). Solution A was added to solution B and subjected to a 50 W ultrasonic vibration for 2 min. The mixture was allowed to rest for 24 h in a saturated atmosphere of isopropyl alcohol. Finally, the resulting gel was dried at 110 °C for 16 h and then calcined at 450, 650, and 850 °C for 16 h in air. The prepared powder samples were called  $\text{TiO}_2$ ,  $\text{Ti}_{0.91}\text{O}_{1.91}\text{Cu}_{0.09}$ ,  $\text{Ce}_{0.09}\text{Ti}_{0.82}\text{O}_{1.91}\text{Cu}_{0.09}$ , and  $\text{Ce}_{0.27}\text{Ti}_{0.64}\text{O}_{1.91}\text{Cu}_{0.09}$ , expressing the amount of each component as atomic fractions.

**Sample Characterizations.** **(a) Physical Absorption Measurements.**  $\text{N}_2$  adsorption/desorption measurements were carried out at liquid  $\text{N}_2$  temperature in a Micromeritics AccuSorb 2100E instrument. The specific surface area (BET) and the pore size were measured using the adsorption and desorption branches, respectively. Prior to measuring, all the samples were degassed at 250 °C for 16 h and finally outgassed to  $10^{-4}$  Pa.

**(b) X-ray Diffraction Study.** The X-ray powder diffraction patterns were obtained using an automatic Rigaku Rotaflex model RU 200B diffractometer with  $\text{Cu K}\alpha$  radiation (40 kV/40 mA, 1.5405 Å) and a graphite monochromator. The scanning range was 20–60° ( $2\theta$ ) with a step size of 0.02° and a step time of 3.0 s. The identification of crystalline phases was accomplished by comparison with JCPDS files numbers 21-1272, 21-1276, 43-1002, and 41-254 for anatase and rutile phases and cerium and copper oxides, respectively.

**(c) Raman Spectroscopy.** The spectra were recorded on a triple Jobin-Yvon T64000 Raman instrument equipped with a microscope and a CCD detection system. The spectra were obtained at room temperature using the 5145 Å line of an argon ion laser (model Spectra Physics 2020) excited with an incident power of 50 mW.

## Results

**Specific Surface Area ( $S_{\text{BET}}$ )– $\text{N}_2$  Adsorption.** Table 1 gives the surface area and pore size of the several titanium oxides, pure and after the addition of copper oxide and cerium oxide, after being calcined at two different temperatures, 450 and 650 °C.

According to the results presented in Table 1, the BET area of the samples was strongly dependent on the thermal treatment temperature and on cerium oxide addition. When the  $\text{TiO}_2$  and  $\text{Ti}_{0.91}\text{O}_{1.91}\text{Cu}_{0.09}$  samples were calcined at 650 °C, the surface area was measured as being equal to 15 and 10  $\text{m}^2/\text{g}$ , respectively, which corresponds to a decrease of 81% and 88%, when compared to the samples calcined at 450 °C.  $\text{Ce}_{0.09}\text{Ti}_{0.82}\text{O}_{1.91}\text{Cu}_{0.09}$  and  $\text{Ce}_{0.27}\text{Ti}_{0.64}\text{O}_{1.91}\text{Cu}_{0.09}$  samples treated at 450

**Table 1. BET Surface Area ( $S$ ), Pore Size (PS), and the Crystallographic Phases Observed by XRD and Raman Spectroscopy of  $\text{TiO}_2$ ,  $\text{CuO–TiO}_2$ , and  $\text{CuO/CeO}_2\text{–TiO}_2$  Samples Calcined at 450 and 650 °C**

samples	$T = 450\text{ }^\circ\text{C}$			$T = 650\text{ }^\circ\text{C}$		
	$S/\text{m}^2\text{ g}^{-1}$	PS/ nm	phase <sup>a</sup>	$S/\text{m}^2\text{ g}^{-1}$	PS/ nm	phase <sup>a</sup>
$\text{TiO}_2$	79	20.2	a	15	—	a/r
$\text{Ti}_{0.91}\text{O}_{1.91}\text{Cu}_{0.09}$	84	35.0	a	10	—	r, t
$\text{Ce}_{0.09}\text{Ti}_{0.82}\text{O}_{1.91}\text{Cu}_{0.09}$	124	18.4	a, c	61	43.0	a/r, c, t
$\text{Ce}_{0.27}\text{Ti}_{0.64}\text{O}_{1.91}\text{Cu}_{0.09}$	105	18.7	a, c	51	58.1	a/r, c, t

<sup>a</sup> (a) anatase and (r) rutile  $\text{TiO}_2$  phases; (c) cerianite  $\text{CeO}_2$  phase; (t) tenorite  $\text{CuO}$  phase.

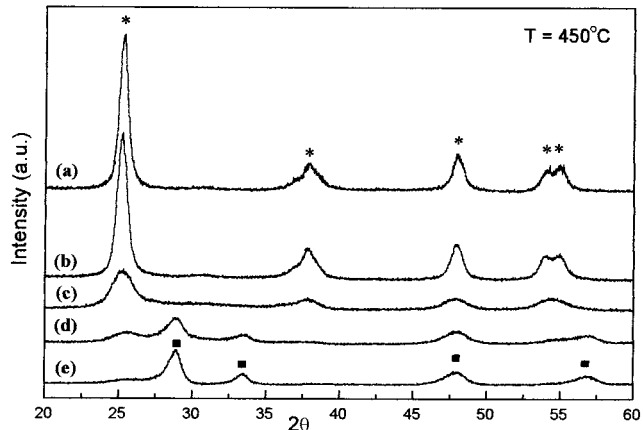


**Figure 1.** XRD patterns of samples calcined at 450 °C: (a)  $\text{TiO}_2$ , (b)  $\text{Ti}_{0.91}\text{O}_{1.91}\text{Cu}_{0.09}$ , (c)  $\text{Ce}_{0.09}\text{Ti}_{0.82}\text{O}_{1.91}\text{Cu}_{0.09}$ , and (d)  $\text{Ce}_{0.27}\text{Ti}_{0.64}\text{O}_{1.91}\text{Cu}_{0.09}$ . (\*) fase  $\text{TiO}_2$  anatase, (+) fase  $\text{TiO}_2$  rutile, (■) fase  $\text{CeO}_2$  cerianite.

°C present higher surface. After the calcination at 650 °C, an average surface area around 55  $\text{m}^2/\text{g}$  was found, which corresponds to a decrease of 49%. All the samples calcined at 850 °C presented a surface area smaller than 8  $\text{m}^2/\text{g}$ , which is the reliable inferior limit of the equipment.

Concerning the pore size (Table 1), for the samples calcined at 450 °C, we observed that the pore size increases from about 20 nm for the  $\text{TiO}_2$  sample to about 35 nm for the  $\text{Ti}_{0.91}\text{O}_{1.91}\text{Cu}_{0.09}$  sample. However, when  $\text{CeO}_2$  was added to the sample, we observed a decrease in the pore size value to about 18 nm. When the samples were calcined at 650 °C, for the  $\text{TiO}_2$  and  $\text{Ti}_{0.91}\text{O}_{1.91}\text{Cu}_{0.09}$  samples, it was not possible to distinguish peaks in the pore size distribution curves for the range analyzed (10–300 Å). Concerning the other two samples, the pore sizes of the two samples containing cerium oxide increase to values around 43 and 58 nm. These results show that the addition of  $\text{CeO}_2$  to the  $\text{TiO}_2$  and  $\text{Ti}_{0.91}\text{O}_{1.91}\text{Cu}_{0.09}$  samples stabilizes their textural structure, hindering agglomeration and thus preventing pore growth. The dependence of the pore size on the temperature of calcination is corroborated by the decrease of the BET area.

**X-ray Diffraction Analysis.** Table 1 reports the crystallographic phases observed by XRD analysis.

The XRD results for  $\text{CuO}/\text{TiO}_2$  and  $\text{CuO–CeO}_2/\text{TiO}_2$  calcined at 450 °C (Figure 1) revealed the presence of  $\text{TiO}_2$ –anatase and  $\text{CeO}_2$ –cerianite.<sup>24</sup> The amount of these phases depends on the  $\text{TiO}_2/\text{CeO}_2$  composition and does not depend on the copper oxide content. A significant change in the XRD patterns of anatase phase ( $\text{TiO}_2$

- (21) Larsson, P.-O.; Andersson, A. *J. Catal.* **1998**, 179, 72.
- (22) Trovarelli, A.; Zamar, F.; Lorca, J.; Leitenburg, C.; Kiss, J. T. *J. Catal.* **1997**, 169, 490.
- (23) Francisco, M. S. P.; Mastelaro, V. R.; Florentino, A. O.; Bazin, D. *Top. Catal.*, in press.

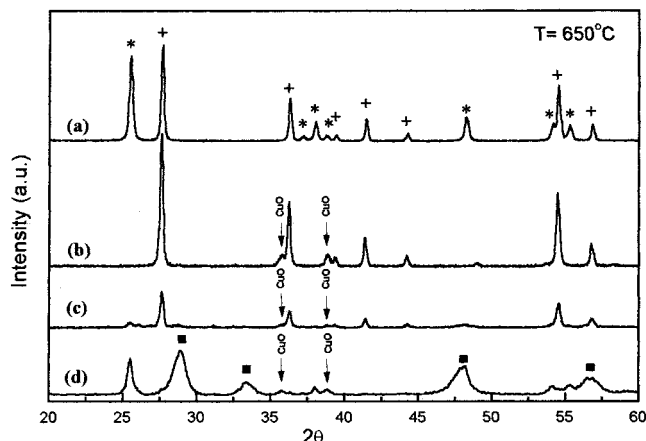


**Figure 2.** XRD patterns of samples calcined at 650 °C: (a)  $\text{TiO}_2$ , (b)  $\text{Ti}_{0.91}\text{O}_{1.91}\text{Cu}_{0.09}$ , (c)  $\text{Ce}_{0.09}\text{Ti}_{0.82}\text{O}_{1.91}\text{Cu}_{0.09}$ , and (d)  $\text{Ce}_{0.27}\text{Ti}_{0.64}\text{O}_{1.91}\text{Cu}_{0.09}$ . (\*) fase  $\text{TiO}_2$  anatase, (+) fase  $\text{TiO}_2$  rutile, (■) fase  $\text{CeO}_2$  cerianite.

sample, Figure 1a) took place after the addition of ceria. In this situation, diffraction peaks of anatase– $\text{TiO}_2$  became broadened, and the diffraction peaks of ceria can be clearly observed ( $\text{Ce}_{0.09}\text{Ti}_{0.82}\text{O}_{1.91}\text{Cu}_{0.09}$  sample, Figure 1c). For the  $\text{Ce}_{0.27}\text{Ti}_{0.64}\text{O}_{1.91}\text{Cu}_{0.09}$  sample (Figure 1d), only the main peak of the  $\text{TiO}_2$  anatase phase, ca. 25.4° ( $2\theta$ ), was barely observable. Furthermore, no solid solution was identified since no significant peak shift of the above-mentioned diffraction peaks was observed.

Figure 2 shows the diffractograms of the samples calcined at 650 °C. The diffractogram of the  $\text{TiO}_2$  reference compound (Figure 2a) presents two crystalline phases: anatase and rutile. When copper oxide was added to  $\text{TiO}_2$  (Figure 2b), only the rutile phase was identified and the  $\text{CuO}$  phase was barely observed. After the addition of cerium oxide (Figure 2c), the diffraction peaks of the  $\text{TiO}_2$  rutile phase became smaller and the peaks related to the anatase and the  $\text{CuO}$  phases practically disappear. As indicated in Figure 2d, in the  $\text{Ce}_{0.27}\text{Ti}_{0.64}\text{O}_{1.91}\text{Cu}_{0.09}$  sample, the X-ray diffraction pattern showed the presence of  $\text{TiO}_2$  anatase and  $\text{CeO}_2$  cerianite phases and few peaks related to the  $\text{CuO}$  phase.

The XRD patterns of the samples calcined at 850 °C are shown in Figure 3. In all samples, we observed the presence of the  $\text{TiO}_2$  rutile phase. In the samples that also contain cerium and copper oxides, we observed the presence of  $\text{CeO}_2$  cerianite and  $\text{CuO}$  phases. In no sample calcined at this temperature did we observe the presence of the  $\text{TiO}_2$  anatase phase.

**Raman Spectroscopy Data.** Raman spectroscopy was also employed to study the structure of the samples. Table 1 summarizes the crystallographic phases observed by Raman spectroscopy, which are in agreement with the XRD results.

Raman spectroscopy of samples calcined at 450 °C (Figure 4) revealed the presence of only two crystalline phases,  $\text{TiO}_2$  anatase and  $\text{CeO}_2$  cerianite, indicating a good dispersion of copper species.<sup>26</sup>

The Raman spectra of the samples calcined at 650 °C are shown in Figure 5. The Raman spectrum of a

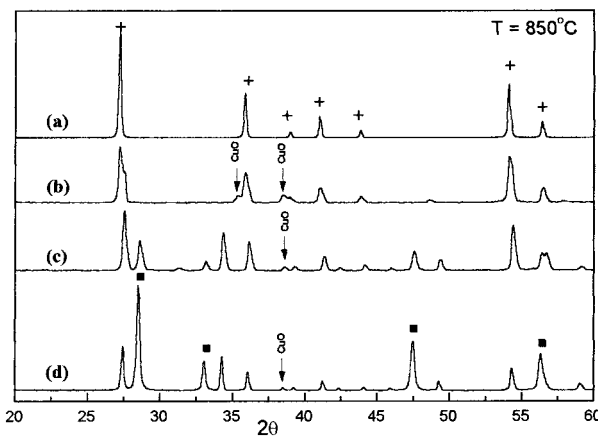


**Figure 3.** XRD patterns of samples calcined at 850 °C: (a)  $\text{TiO}_2$ , (b)  $\text{Ti}_{0.91}\text{O}_{1.91}\text{Cu}_{0.09}$ , (c)  $\text{Ce}_{0.09}\text{Ti}_{0.82}\text{O}_{1.91}\text{Cu}_{0.09}$ , and (d)  $\text{Ce}_{0.27}\text{Ti}_{0.64}\text{O}_{1.91}\text{Cu}_{0.09}$ . (+) fase  $\text{TiO}_2$  rutile, (■) fase  $\text{CeO}_2$  cerianite.

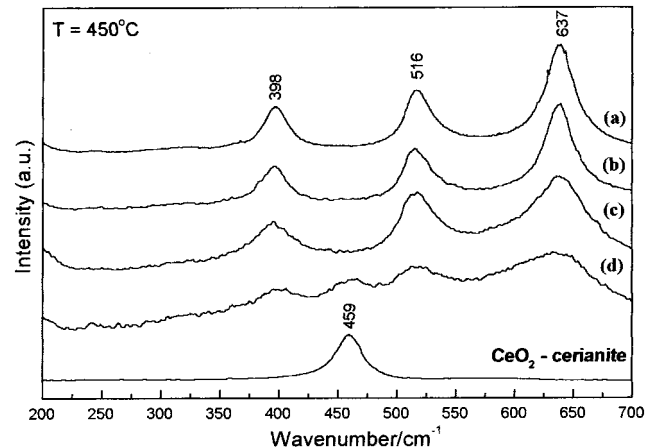


**Figure 4.** FT-Raman spectra of samples calcined at 450 °C: (a)  $\text{TiO}_2$ , (b)  $\text{Ti}_{0.91}\text{O}_{1.91}\text{Cu}_{0.09}$ , (c)  $\text{Ce}_{0.09}\text{Ti}_{0.82}\text{O}_{1.91}\text{Cu}_{0.09}$ , and (d)  $\text{Ce}_{0.27}\text{Ti}_{0.64}\text{O}_{1.91}\text{Cu}_{0.09}$ .

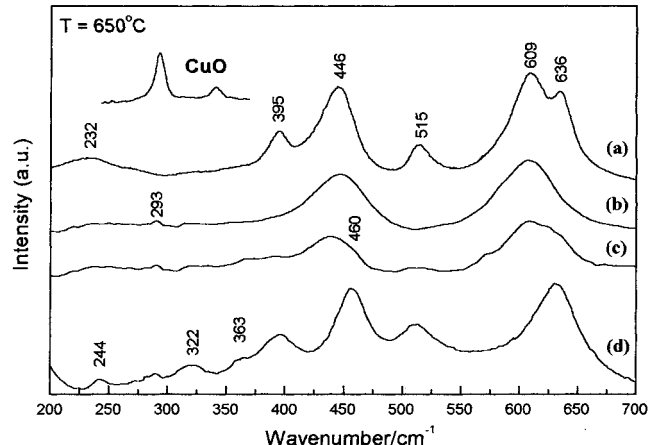


**Figure 5.** FT-Raman spectra of samples calcined at 650 °C: (a)  $\text{TiO}_2$ , (b)  $\text{Ti}_{0.91}\text{O}_{1.91}\text{Cu}_{0.09}$ , (c)  $\text{Ce}_{0.09}\text{Ti}_{0.82}\text{O}_{1.91}\text{Cu}_{0.09}$ , and (d)  $\text{Ce}_{0.27}\text{Ti}_{0.64}\text{O}_{1.91}\text{Cu}_{0.09}$ .

pure  $\text{TiO}_2$  sample (Figure 5a) reveals six strong Raman bands. Three bands at 232, 446, and 609  $\text{cm}^{-1}$  are in agreement with data observed in the spectra of a rutile phase,<sup>4,25</sup> the other three bands, at 395, 515, and 636  $\text{cm}^{-1}$ , are observed in the spectra of anatase phase.

(24) Francisco, M. S. P.; Nascente, P. A. P.; Mastelaro, V. R.; Florentino, A. O. *J. Vac. Sci. Technol. A* **2001**, *19*, 1150.

(25) Wu, M.; Zhang, W.; Du, Z.; Huang, Y. *Mod. Phys. Lett. B* **1999**, *13*, 167.

(26) Francisco, M. S. P.; Nascente, V. R.; Florentino, A. O. *J. Phys. Chem. B* **2001**, *105*, 10515.

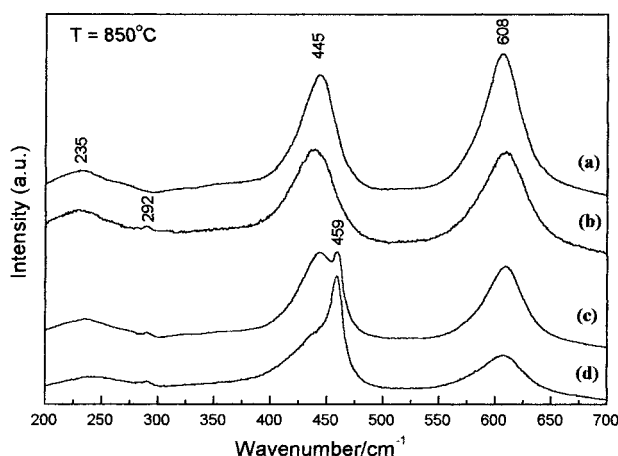


**Figure 6.** FT-Raman spectra of samples calcined at 850 °C: (a)  $\text{TiO}_2$ , (b)  $\text{Ti}_{0.91}\text{O}_{1.91}\text{Cu}_{0.09}$ , (c)  $\text{Ce}_{0.09}\text{Ti}_{0.82}\text{O}_{1.91}\text{Cu}_{0.09}$ , and (d)  $\text{Ce}_{0.27}\text{Ti}_{0.64}\text{O}_{1.91}\text{Cu}_{0.09}$ .

These modes correspond to the fundamental modes for these phases.<sup>2,4,25</sup> The peak at  $232\text{ cm}^{-1}$  is assigned to a disordered-induced scattering mode of rutile.<sup>4</sup> After the addition of  $\text{CuO}$  to  $\text{TiO}_2$  ( $\text{Ti}_{0.91}\text{O}_{1.91}\text{Cu}_{0.09}$  sample, Figure 5b), the Raman lines related to the anatase phase disappear, and only two broad bands at 446 and  $609\text{ cm}^{-1}$  which correspond to the rutile phase were identified. When cerium oxide is added to the  $\text{Ti}_{0.91}\text{O}_{1.91}\text{Cu}_{0.09}$  sample ( $\text{Ce}_{0.09}\text{Ti}_{0.82}\text{O}_{1.91}\text{Cu}_{0.09}$  sample, Figure 5c), the two Raman bands ascribed to the rutile phase are still observed in the spectrum, however, accompanied by the appearance of the three Raman lines at 395, 515, and  $636\text{ cm}^{-1}$  ascribed as being anatase phase. The typical strong line of cerium oxide at  $460\text{ cm}^{-1}$  is barely recognizable as a shoulder on the rutile bands, and it is due to the Raman-active mode characteristic of fluorite-structured materials.<sup>21,27</sup> In the spectrum of the sample with the highest amount of cerium oxide ( $\text{Ce}_{0.27}\text{Ti}_{0.64}\text{O}_{1.91}\text{Cu}_{0.09}$  sample, Figure 5d) the band of ceria at  $460\text{ cm}^{-1}$  was easily identified while no rutile band was observed. However, in addition to the anatase fundamentals at 395, 515, and  $636\text{ cm}^{-1}$ ,<sup>3,25</sup> this spectrum showed a great number of smaller bands which do not correspond to the Raman modes in single-crystal and polycrystalline anatase. The  $244\text{ cm}^{-1}$  mode was frequently observed in nanophase  $\text{TiO}_2$  whereas the modes at 322 and  $363\text{ cm}^{-1}$  have been associated with defects in the  $\text{TiO}_2$  nanocrystalline phase.<sup>25</sup>

Figure 6 presents the Raman spectra of the samples calcined at 850 °C. At this temperature, only the bands of the  $\text{TiO}_2$  rutile phase were identified, except for the band at  $445\text{ cm}^{-1}$  in the spectrum of the  $\text{Ce}_{0.27}\text{Ti}_{0.64}\text{O}_{1.91}\text{Cu}_{0.09}$  sample, in which we can observe a shoulder related to the presence of the  $\text{CeO}_2$  crystalline phase. The Raman line at  $459\text{ cm}^{-1}$  of  $\text{CeO}_2$  was easily distinguished, even for the spectrum of the sample with the least amount of  $\text{CeO}_2$  ( $\text{Ce}_{0.09}\text{Ti}_{0.82}\text{O}_{1.91}\text{Cu}_{0.09}$  sample, Figure 6c).

All the samples containing copper oxide and calcined at 650 and 850 °C presented a band near  $293\text{ cm}^{-1}$ , which has been reported by other authors as due to the  $\text{CuO}$  crystalline phase.<sup>27,28</sup>

## Discussion

**TiO<sub>2</sub> and Ti<sub>0.91</sub>O<sub>1.91</sub>Cu<sub>0.09</sub> Samples.** According to Ramis et al.,<sup>29</sup> the anatase phase transforms into the rutile phase at 700 °C, and such a transformation will be complete at 800 °C. The sol–gel method when processed in highly acid conditions induces hydrolysis of titanium alkoxide at a faster rate than is the condensation, producing samples with many hydroxyls.<sup>30</sup> The presence of these hydroxyl groups produces defects in the framework, which are titanium and oxygen vacancies.<sup>30</sup> These defects are responsible for promoting the anatase–rutile transformation in a lower temperature, explaining the presence of the rutile phase in pure  $\text{TiO}_2$  calcined at 650 °C (Figures 2–5a), together with the anatase phase.

The XRD and Raman patterns of the  $\text{Ti}_{0.91}\text{O}_{1.91}\text{Cu}_{0.09}$  sample calcined at 650 °C (Figures 2–5b) showed that copper oxide probably catalyzes the mass transport to the nucleation region of rutile phase (with higher mass density), promoting rutile nuclei growth, thus favoring the phase transition. The mass movement can be thought as the removal of the defects in excess formed during the sol–gel process from the nucleation region. Likely,  $\text{CuO}$  is responsible for a higher number of defects inside the anatase phase, in such a way that formation and growth of a higher number of rutile nuclei into  $\text{TiO}_2$  anatase take place faster.

Some works have been reported on the modification of the anatase–rutile phase transformation when copper oxide is used as a dopant; it was concluded that the mechanism responsible for such a modification is an excess of oxygen vacancies that accelerates the transition and the crystallite growth.<sup>16,31,32</sup>

Nair et al.<sup>31</sup> studied the microstructure and phase transformation behavior of doped nanostructured titania. According to this work,  $\text{CuO}$  and  $\text{NiO}$  enhanced the anatase transformation and the sintering. On the other hand,  $\text{La}_2\text{O}_5$  retarded both transformation and densification. Dopants with an oxidation state above 4+ will reduce the oxygen vacancy concentration in the titania lattice as an interstitial impurity. Dopants with an oxidation state of 3+ or lower are placed in the titania lattice points, creating a charge-compensating anion vacancy.

The anatase–rutile transformation involves an overall contraction of the oxygen structure and a cooperative movement of ions.<sup>9</sup> It is not easy to obtain a conclusion about a link between anatase–rutile transformation and crystallite growth, but it is very well-known that the phase transformation and sintering behaviors are interrelated.

Our the BET surface area, XRD and Raman spectroscopy results for  $\text{TiO}_2$  and  $\text{Ti}_{0.91}\text{O}_{1.91}\text{Cu}_{0.09}$  samples are in good agreement with the statements discussed above. The addition of  $\text{CuO}$  to  $\text{TiO}_2$  was responsible for

(28) Reimann, K.; Syassen, K. *Solid State Commun.* **1990**, *76*, 137.

(29) Ramis, G.; Busca, G.; Cristiani, C.; Liette, L.; Forzatti, P.; Bregani, F. *Langmuir* **1992**, *8*, 1744.

(30) López, T.; Gómez, R.; Pecci, G.; Reyes, P.; Bokhimi; Novaro, O. *Mater. Lett.* **1999**, *40*, 59.

(31) Nair, J.; Nair, P.; Mizukami, F.; Oosawa, Y.; Okubo, T. *Mater. Res. Bull.* **1999**, *34*, 1275.

(32) Yuan, S.; Mériadeau, P.; Perrichon, V. *Appl. Catal., B* **1994**, *3*, 319.

accelerating the  $\text{TiO}_2$  phase transformation and its crystal growth.

**CuO–CeO<sub>2</sub>/TiO<sub>2</sub> Samples.** As we discussed before, it is known that the anatase–rutile transformation is related to many factors, such as impurities present in anatase, preparation conditions, precursors, dopants, morphology of the particles, and others. Lin et al.<sup>33</sup> studied the influence of adding dopants in the anatase–rutile transition temperature. In their work, XRD results of mixtures of  $\text{TiO}_2$  with rare earth oxides (0.5 wt %) revealed that the presence of these oxides can inhibit the phase transformation during the thermal treatment, even with mixtures calcined at moderately high temperatures ( $\leq 650$  °C for  $\text{TiO}_2/\text{La}_2\text{O}_3$ ,  $\leq 700$  °C for  $\text{TiO}_2/\text{Y}_2\text{O}_3$  or  $\text{CeO}_2$ ). The inhibition of the transition was ascribed to the stabilization of the anatase phase by the surrounding rare earth oxides through the formation of Ti–O–rare earth element bonds. At the interface, titanium atoms substituted the rare earth elements in the lattice of the rare earth oxides to form tetragonal Ti sites. The interaction between the different tetrahedral Ti atoms (in  $\text{La}_2\text{O}_3$  and  $\text{Y}_2\text{O}_3$ ) or between the tetrahedral Ti and octahedral Ti (in  $\text{CeO}_2$ ) inhibits the phase transformation.

A similar explanation was offered for the inhibition of the phase transformation for a  $\text{TiO}_2/\text{SiO}_2$  mixture (ratio 30/70).<sup>34</sup> The stabilization of the anatase phase takes place by the surrounding  $\text{SiO}_2$  phase through the  $\text{TiOSi}$  interface. At the interface,  $\text{TiO}_2$  atoms are substituted into the tetrahedral  $\text{SiO}_2$  lattice forming a tetrahedral Ti site. The interaction between the tetrahedral Ti species and the octahedral Ti sites in the anatase is thought to prevent the transformation to rutile. The  $\text{SiO}_2$  lattice locks the Ti–O species at the interface with the  $\text{TiO}_2$  domains preventing the nucleation that is necessary for anatase transformation to rutile.

The XRD and Raman results of the  $\text{Ce}_{0.09}\text{Ti}_{0.82}\text{O}_{1.91}\text{Cu}_{0.09}$  and  $\text{Ce}_{0.27}\text{Ti}_{0.82}\text{O}_{1.91}\text{Cu}_{0.09}$  samples calcined at 650 °C (Figures 2–5c,d) showed that the likely formation of Ce–O–Ti interaction took place, inhibiting the transition of the  $\text{TiO}_2$  phase. The Ce–O–Ti interaction blocks the Ti–O species at the interface with  $\text{TiO}_2$  domains stabilizing them, hiding the agglomeration of  $\text{TiO}_2$  and thus preventing their growth. Moreover, the cerium oxide-modified  $\text{TiO}_2$  support, in combination with the presence of CuO, promoted greater methanol conversion than the catalyst using a pure  $\text{TiO}_2$  support ( $\text{Ti}_{0.91}\text{O}_{1.91}\text{Cu}_{0.09}$  sample), indicating a synergistic effect between CuO and the  $\text{CeO}_2$ – $\text{TiO}_2$  mixed support.<sup>23,24</sup>

Our results are in general agreement with data from the literature. The catalytic combustion of diesel soot particles on copper catalysts supported on  $\text{TiO}_2$  was enhanced by the presence of potassium.<sup>32</sup> The effect was attributed to the formation of mixed K–Ti oxides which inhibit the sintering of the  $\text{TiO}_2$  support and thus increased the surface area of the catalysts. Titania modified with 3 and 12  $\mu\text{mol}$   $\text{Ce}/\text{m}^2$  surface area of the titania (173  $\text{m}^2/\text{g}$ ) was used as support for copper oxides.<sup>21</sup>  $\text{CeO}_2$  added to the CuO/ $\text{TiO}_2$  system stabilized the surface area of the  $\text{TiO}_2$  support in the presence of copper oxide.

The decrease of crystallite sizes<sup>23</sup> and the inhibition of titania phase transformation with the addition of cerium oxide are consistent with the increase of surface area and the inhibition of the sintering of supports with added cerium oxide. All these results indicate the addition of  $\text{CeO}_2$  to the matrix modifies the mechanism of formation of the titania phases.

The proposed model for CuO/CeO<sub>2</sub>– $\text{TiO}_2$ , previously reported,<sup>23,24</sup> corroborate our present data and the literature. The model proposed for cerium oxide-modified  $\text{TiO}_2$  support was well supported by the XPS results, which showed a second Ti atom species in a distorted structure after the addition of cerium oxide.<sup>24</sup> Moreover, EXAFS measurements at the Ce L<sub>III</sub>-edge also revealed that, in sample catalysts containing 9% of cerium oxide, the cerium atoms presented a well-distorted local structure, which could also indicate an interaction between Ce, Ti, and Cu atoms.<sup>23</sup>

Yang et al.<sup>35–37</sup> studied the effects of different  $\text{TiO}_2$  modifiers in the anatase–rutile transformation. For  $\text{ZrO}_2$ -containing samples (a system with Zr/Ti molar rate of 0.10), the DTA curve (differential thermal analysis) indicated an exothermic peak assigned to the anatase–rutile transition at 1100 °C.<sup>35</sup> The same peak were observed at 973 °C in the DTA curve of the  $\text{TiO}_2$  added with  $\text{Al}_2\text{O}_5$  (Al/Ti molar rate of 0.10).<sup>36,37</sup> In both systems, the authors suggested that the formation of a metastable anatase solid solution containing alumina and a solid solution of  $\text{ZrO}_2$  in anatase at low temperature are responsible for the higher anatase–rutile transition temperature. Comparing these results with our data for the  $\text{Ce}_{0.09}\text{Ti}_{0.82}\text{O}_{1.91}\text{Cu}_{0.09}$  sample, it seems that the effect of the ceria loading in the  $\text{CeO}_2/\text{TiO}_2$  matrix is moderated. Nevertheless, these authors analyzed the  $\text{Al}_2\text{O}_5/\text{TiO}_2$  and  $\text{ZrO}_2/\text{TiO}_2$  samples after a thermal treatment for 1 h, while our analyses were performed in samples thermally treated for 16 h.

## Conclusions

The phase transformation and the sintering behavior of titania have been studied with the objective to better understand the effect of the addition of  $\text{CeO}_2$  and CuO dopants. It has been found that the CuO dopant accelerates the anatase–rutile transition and also assists the sintering process. Copper-doped samples also sintered to near-zero porosity at 650 °C. The addition of  $\text{CeO}_2$  to the CuO/ $\text{TiO}_2$  system increased specific surface area of the mixed oxide and prevented the sintering of samples calcined at higher temperature. At the same time this prevented pore size growth and the titania phase transformation.

**Acknowledgment.** The research work was partially performed at the Grupo de Propriedades Ópticas (GPO) of the IFGW-UNICAMP, Brazil. The authors acknowledge Prof. Carol H. Collins (IQ-UNICAMP) for manuscript revision. This work was supported by the Brazilian research funding institutions FAPESP and CNPq.

CM011520B

(35) Yang, J.; Ferreira, J. M. F. *Mater. Res. Bull.* **1998**, 33, 389.

(36) Yang, J.; Ferreira, J. M. F. *Mater. Lett.* **1998**, 36, 320.

(37) Yang, J.; Huang, Y. X.; Ferreira, J. M. F. *J. Mater. Sci., Lett.* **1997**, 16, 1933.